The N=14 shell closure in ^{22}O viewed through a neutron sensitive probe

E. Becheva, Y. Blumenfeld, E. Khan, D. Beaumel, J.M. Daugas, F. Delaunay, C.E. Demonchy, A. Drouart, M. Fallot, A. Gillibert, et al.

The N=14 shell closure in ^{22}O viewed through a neutron sensitive probe

E. Becheva[a)], Y. Blumenfeld[a)], E. Khan[a)], D. Beaumel[a)], J.M. Daugas[b)], F. Delaunay[a)], Ch-E. Demonchy[c)], A. Drouart[d)], M. Fallot[a)], A. Gillibert[d)], L. Giot[c)], M. Grasso[a),e)], N. Keeley[d)], K.W. Kemper[f)], D. T. Khoa[g)], V. Lapoux[d)], V. Lima[a)], A. Musumarra[e)], L. Nalpas[d)], E.C. Pollacco[d)], O. Roig[b)], P. Roussel-Chomaz[c)], J.E. Sauvestre[b)], J.A. Scarpaci[a)], F. Skaza[d)], H. S. Than[g)]

a) Institut de Physique Nucléaire, IN$_2$P$_3$-CNRS, 91406 Orsay, France
b) DPTA/SPN-CEA Bruyères, 91680 Bruyères-le-Châtel Cedex 12,France
c) GANIL (CEA/DSM-CNRS/IN$_2$P$_3$), BP 5027, 14076 Caen Cedex, France
d) SPhN, DAPNIA, CEA Saclay, 91191 Gif sur Yvette Cedex, France
e) INFN-Laboratorio Nazionale del Sud, Via S. Sofia 44, Catania, Italy
f) Department of Physics, Florida State University, Tallahassee, FL-32306, USA
g) INST, Vietnam Atomic Energy Commission, P.O. Box 5T-160, Nghia Do, Hanoi, Vietnam

(Dated: September 21, 2005)

To investigate the behavior of the N=14 neutron gap far from stability with a neutron-sensitive probe, proton elastic and 2_1^+ inelastic scattering angular distributions for the neutron-rich nucleus ^{22}O were measured with a secondary beam intensity of only 1200 particles per second using the MUST silicon strip detector array at the GANIL facility. A phenomenological analysis yields a deformation parameter $\beta_{p,p'} = 0.26 \pm 0.04$ for the 2_1^+ state, much lower than in ^{20}O, showing a surprisingly weak neutron contribution to this state. A fully microscopic analysis was performed using optical potentials obtained from matter and transition densities generated by continuum Skyrme-HFB and QRPA calculations, respectively. When the present results and those from a ^{22}O + ^{197}Au scattering experiment are combined, the ratio of neutron to proton contributions to the 2_1^+ state is found close to the N/Z ratio, demonstrating a strong N=14 shell closure in the vicinity of the neutron drip-line.

PACS numbers: 21.10.Re, 25.40.Cm, 25.40.Ep, 21.60.Jz, 24.10.Eq

Shell structure is a distinctive feature of many-body fermionic systems, such as metallic clusters, atoms and nuclei [1–3]. Such structure is characterized by the existence of magic numbers. Nuclei are composed of two types of interacting fermions, giving rise to a specific degree of freedom, isospin. Therefore, there are magic numbers for both neutrons and protons, which are in principle the same if charge independence holds. An important question, specific to nuclear physics, is the robustness of the shell closures as a function of neutron to proton asymmetry: an eventual modification of magic numbers far from stability could have major implications on our understanding of nucleosynthesis through the r and rp processes, as nuclear structure is an important input to the models of explosive astrophysical scenarios [4]. Theoretical predictions for the disappearance of well-known magic numbers and the appearance of new shell gaps far from stability have recently been given [5, 6]. With the advent of radioactive beams during the last decade, experimental indications of such a behavior have emerged (see e.g. [7]) for neutron magic numbers. However the neutron gap is usually measured with an exclusively proton sensitive probe, such as Coulomb excitation. Only indirect information on the neutron gap evolution is obtained, through the neutron-proton interaction. Complementary probes are therefore necessary to investigate the neutron behavior. The purpose of this Letter is to give for the first time experimental evidence for a new neutron magic number using a probe mainly sensitive to neutrons.

In this context, one of the most studied areas is the neutron-rich part of the oxygen isotopic chain which has a well-established proton magic number Z=8: many experimental [8–11] and theoretical [5, 12–14] efforts have been devoted to the $^{18-24}$O isotopes, showing possible N=14 and N=16 shell closures, which would make both ^{22}O and ^{24}O doubly magic nuclei. The energy of the first 2_1^+ state of ^{22}O has been measured at 3199(8) keV [9], compared to 1670 keV in ^{20}O, and its small B(E2) value of 21(8) e^2·fm^4 [10] indicates a strengthening of the N=14 shell gap. Even though the 2_1^+ state of ^{24}O has not been directly observed, its energy has been shown to lie above 3.8 MeV, indicating an N=16 shell closure [11]. Conversely, ^{28}O, which is doubly magic in the standard shell model, was found to be unbound [15], contrary to most theoretical predictions. Theoretically, both Quasiparticle Random-Phase Approximation (QRPA) [8], and shell model [16] calculations predict a decrease of B(E2) from ^{20}O to ^{22}O. Moreover shell model calculations [6] show a strong gap of 4.3 MeV between the $1d_{5/2}$ and $2s_{1/2}$ subshells, making ^{22}O a magic nucleus.

However, all above mentioned experimental indications of the N=14 magicity in ^{22}O, are partial since they do not probe separately the proton and the neutron contribution to the 2_1^+ excitation. In Ref. [10] the B(E2) value is obtained from inelastic scattering of ^{22}O from ^{197}Au at an energy of 50 MeV/nucleon. The deduced B(E2) value provides the proton transition matrix element M_p

but since both Coulomb and nuclear interactions were important in the reaction, the authors had to rely on theoretical predictions to isolate the neutron and proton contributions to the excitation. In other words, in the absence of data from a second experimental probe, the B(E2) value is model-dependent. Moreover, it is somewhat delicate to interpret the neutron gap behavior using the B(E2) values which depend only on the proton contribution to the excitation : as stated above, the neutron gap is probed through the neutron-proton interaction, the knowledge of which is subject to debate close to the neutron drip-line [5, 17].

The neutron and proton transition matrix elements $M_{n,p} =< 2^+|r^2Y_{20}|0^+ >$ of a quadrupole operator are obtained by integrating the corresponding transition densities $\delta\rho_{n,p}(r)$ over r. In this case the proton transition matrix element M_p is related to the reduced transition probability by B(E2)=M_p^2. B(E2) must be measured through an electromagnetic experiment. To disentangle the proton (M_p) and the neutron (M_n) transition matrix elements of the 2_1^+ excitation in ^{22}O, we make use of a (p,p') scattering experiment on ^{22}O. This second experimental probe, complementary to the ^{197}Au target, should allow us to deduce a model-independent value of B(E2), and to evaluate the neutron contribution to the excitation. The combined data probe more directly the possible N=14 shell closure.

Protons at a few tens of MeV are known to interact three times more strongly with neutrons than with protons in the nucleus [18], whereas Coulomb excitation or lifetime measurements probe directly only the proton density distributions. The combination of the two types of measurements can therefore disentangle proton and neutron contributions to excited states. With the development of radioactive beams, proton scattering data can now be obtained for unstable nuclei. Elastic and inelastic proton scattering experiments on ^{20}O were recently performed [8, 19], indicating a large isovector component in the excitation of the 2_1^+ state, which is driven by the excitation of neutrons. This behavior is characteristic for a single closed-shell nucleus with in this case a partially filled $1d_{5/2}$ sub-shell.

Direct reactions on short-lived unstable nuclei must be performed in inverse kinematics, where a secondary beam of the radioactive nucleus of interest bombards a target containing the light particles [20]. Here the secondary beam was produced by fragmentation of a 77 MeV/nucleon ^{36}S primary beam delivered by the GANIL facility with a power of 1.5 kW on a 540 mg/cm^2 ^{12}C target located between the solenoids of the SISSI device. The secondary beam was selected and purified using the beam analysis spectrometer, equipped with a 150 mg/cm^2 Al achromatic degrader, as a fragment separator. The average intensity on target of the 46.6 MeV/nucleon ^{22}O beam was only 1200 pps with a large contamination of ^{25}Na and ^{23}F, which made up 88% of the beam. The incident nuclei were tracked event-by-event using two low pressure multiwire proportional chambers (CATS) [21]. The reconstructed position resolution on target was approximately 1mm. The secondary beam impinged on a 5 mg/cm^2 polypropylene $(CH_2)_n$ target. In order to select the elastic and inelastic reaction channels the scattered heavy nuclei were identified in the focal plane of the SPEG spectrometer [22]. To gain access to the excitation energy and the scattering angle characterizing the reaction, the energy and angle of the recoiling protons were measured using the MUST array [23], consisting of eight silicon-strip detectors, backed by Si(Li) diodes and CsI crystals. Protons were unambiguously identified through a combination of energy, energy-loss and time-of-flight measurements. The trigger condition was given by a coincidence between the SPEG plastic detector and the MUST array, which, combined with the off-line proton and ^{22}O identification, effectively reduced the background from the carbon component of the target.

Figure 1a) shows the scatterplot of the proton laboratory angle vs. energy for ^{22}O, where kinematic lines corresponding to the ground and 2_1^+ states are very well separated. Fig. 1b) displays the resulting excitation energy spectrum, where the 2_1^+ state is clearly visible at the energy of 3.2 ± 0.2 MeV. No indication for higher lying states is observed. The angular distributions could be obtained directly by selecting the corresponding events in energy. The background is very low as is shown by the absence of significant background to the left of the elastic peak. The absolute normalization was deduced from the number of incident nuclei measured with the CATS detectors and the target thickness. The error on the normalization is estimated to be 10% including the background effect. Fig. 2 displays the measured elastic and 2_1^+ angular distributions. The error bars are purely statistical.

A first approach to understand the results is the so-called phenomenological analysis which makes use of optical potential systematics. The most recent nucleon-nucleus global potential is the parameterization elaborated by Koning and Delaroche (KD) [24] for 24 ≤ A ≤209 nuclei with reaction energies ranging from 2 keV to 200 MeV. We have also performed the analysis using the more familiar Becchetti-Greenlees [25] and CH89 [26] potentials, which yield the same conclusions. Coupled Channel calculations using standard vibrational form factors were performed with the ECIS97 [27] code to obtain inelastic cross sections. The normalization of the inelastic angular distribution to the data leads to the value of the (p,p') deformation parameter $\beta_{(p,p')}$.

The calculated elastic and inelastic angular distributions are displayed in figure 2. An overall good agreement with the data is observed. The extracted deformation parameter is $\beta_{(p,p')}$=0.26 ± 0.04. We have chosen to normalize on the forward data up to 30 deg. Normalizing to the entire angular distribution reduces the β

value by less than 0.01. The error bars correspond to the minimum and maximum $\beta_{(p,p')}$ values which allow the measured angular distributions to be reproduced within the error bars. The $\beta_{(p,p')}$ value of ^{22}O is much smaller than the one measured for ^{20}O ($\beta_{(p,p')}$=0.55 $\pm$ 0.06), and also smaller than for ^{18}O ($\beta_{(p,p')}$=0.37 $\pm$ 0.03) [8]. Since proton scattering is much more sensitive to neutron than to proton excitation, this result clearly indicates a weak neutron contribution to the 2^+_1 excitation in ^{22}O, compared to less neutron-rich isotopes.

Such a simple analysis is valuable for comparison purposes between isotopes, but a more detailed understanding of proton scattering calls for a fully microscopic analysis, totally independent of the phenomenological approach. In the microscopic study performed here, neutron and proton ground state densities are calculated using Skyrme Hartree-Fock-Bogoliubov (HFB) in coordinate space, with the very recently developed exact quasiparticle continuum treatment, the inclusion of which is expected to be important for weakly bound nuclei [29]. The HFB equations are solved in coordinate space assuming spherical symmetry. In the present continuum-HFB calculations the mean field quantities are evaluated using the Skyrme interaction SLy4 [30], while for the pairing interaction we take a zero-range density-dependent force [12].

To describe nuclear transitions, continuum-QRPA calculations are performed using the HFB single quasiparticle spectra. QRPA equations are derived in coordinate space using the linear response theory. For the first time the residual interaction is taken from the second derivative of the HFB energy functional with respect to the matter and pairing densities, together with exact continuum treatment (see [12]).

A measurement of the cross section of the first 2^+ state of ^{22}O was obtained by Thirolf et al. [10] using inelastic scattering from ^{197}Au at 50 MeV/nucleon. However, due to the range of scattering angles covered, both Coulomb and nuclear components are involved in the excitation. We have reanalyzed the data of the ^{22}O+^{197}Au reaction using the same optical potentials as in Ref. [10]. We found that for a given B(E2) value, the calculated excitation cross sections varies very little with respect to the nuclear deformation parameter β_N. Destructive interference between nuclear and Coulomb amplitudes implies that, when the rather large error bar on the cross section [10] is taken into account, the B(E2) value extracted is not sensitive to the nuclear contribution as long as β_N is less than 0.4. The experimental B(E2) from this study is equal to 21 $\pm$ 8 e^2·fm^4. The calculated B(E2) value from QRPA is 22 e^2·fm^4 which agrees well with the measured value, showing that the magnitude of the proton transition density is faithfully reproduced by the theory.

In order to directly compare the model with the proton scattering data, microscopic optical potentials are generated from the HFB and QRPA densities using two different methods: the folding model [31], and a microscopic optical model potential (OMP) parameterization using the JLM interaction [32]. The folding model analysis uses the CDM3Y6 interaction folded with the HFB densities to generate the isoscalar and isovector parts of the OMP. The spin-orbit potential as well as the transition potentials are obtained from the folding of the QRPA transition densities with the nucleon-nucleon interaction. The imaginary part of the OMP is generated with the Koning and Delaroche [24] phenomenological parameterization, already used in our phenomenological analysis above. Cross sections are calculated using DWBA with the ECIS97 [27] code.

The ^{22}O(p,p') angular distributions are displayed in Fig. 2. The elastic angular distribution is well described, even at large angles. Since the B(E2) is well reproduced by the proton transition density, we renormalize the neutron transition density in order to fit the data. This procedure assumes that QRPA reliably describes the shape of the transition density for collective states [28]. It provides an experimental value of the M_n/M_p ratio for the 2^+_1 state, deduced from the combination of the electromagnetic and the (p,p') measurements [8]. We obtain M_n/M_p = 2.5 $\pm$ 1.0, or $(M_n/M_p)/(N/Z)$ = 1.4 $\pm$0.5. This is to be compared to the value for ^{20}O, $(M_n/M_p)/(N/Z) = 2.2 \pm 0.5$, significantly different from 1 [8]. Incidentally, in the case of ^{22}O, the error coming from the heavy ion measurement is greater than from our experiment.

In order to check the dependence on the potential used, complex optical and transition potentials were also obtained by injecting the calculated ground state and transition densities into the Jeukenne, Lejeune and Mahaux (JLM) density dependent optical potential [32], which was derived from Brückner-Hartree-Fock nuclear matter calculations. Cross sections were then calculated in a DWBA approach with the TAMURA code [33]. We have tested that coupling to (p,d) pickup, which can have significant effect on (p,p') scattering of very weakly bound nuclei [34], can be neglected in the present case. Renormalizing the neutron transition density in order to reproduce the inelastic data leads to the same value of the M_n/M_p ratio as when the folding potential is used. Two optical potentials which are known to be reliable yield the same result, which gives confidence that the matter and transition densities are being critically tested here.

The phenomenological analysis points to a small neutron deformation in ^{22}O. The microscopic analysis indicates that protons (Z=8 closed shell) and neutrons contribute in a balanced way to the first 2^+ excitation. This is different from the case of ^{20}O, where the excitation is driven by the neutrons, as expected due to the Z=8 shell closure. The result here, combined with the high energy of the 2^+ state, points to a strong N=14 (sub-)shell closure in neutron rich nuclei. Shell model calculations reported by B.A. Brown [10] using the USD interaction

predict strong N=14 and N=16 gaps in oxygen isotopes. This calculation predicts M_n/M_p=2.6, in agreement with the experimental result.

In summary, the angular distributions for elastic and inelastic scattering to the 2_1^+ state of ^{22}O have been measured using a secondary radioactive beam of only 1200 pps coupled to a highly efficient particle detection system. Proton and neutron contributions to the excitation are disentangled through the comparison of the present results with a heavy ion scattering experiment dominated by electromagnetic excitation. This method is shown to be a general tool to search for neutron shell closures which are only indirectly observed through Coulomb excitation. In the present case evidence for a strong N=14 shell closure is obtained from several independent analyzes. This effect has been predicted by recent shell model calculations. Attention should now turn to ^{24}O and the N=16 sub-shell closure. A successful ^{24}O(p,p') experiment will have to wait for the next generation radioactive beam facilities, but the generality of the present method should allow to enhance our knowledge of neutron shell closure far from stability in regions of heavy nuclei.

We thank P. Gangnant, J.F. Libin and L. Petizon for their expert technical help. The work of K.W.K. was supported by the US National Science Foundation.

[1] P. Leboeuf and A. Monastra, *Ann. Phys.* **297** (2002) 127.
[2] Y. Imry, *Introduction to Mesoscopic Physics* (Oxford, University Press, New York, 1997)
[3] M. Brack, *Rev. Mod. Phys.* **65** (1993) 677.
[4] C. Freiburghaus *et al.*, *Astr. Jour.* **516** (1999) 381.
[5] T. Otsuka *et al.*, *Phys. Rev. Lett* **87** (2001) 082502.
[6] B.A. Brown, *Prog. Part. Nucl. Phys.* **47** (2001) 517
[7] A. Ozawa, T. Kobayashi, T. Suzuki, K. Yoshida, I. Tanihata, *Phys. Rev. Lett* **84** (2000) 5493.
[8] E. Khan *et al.*, *Phys. Lett.* **B490** (2000) 45.
[9] M. Belleguic *et al.*, *Nucl. Phys.* **A682** (2001) 136c.
[10] P.G. Thirolf *et al.*, *Phys. Lett.* **B485** (2000) 16.
[11] M. Stanoiu *et al.*, *Phys. Rev.* **C69** (2004) 034312.
[12] E. Khan, N. Sandulescu, M. Grasso, Nguyen Van Giai, *Phys. Rev.* **C66** (2002) 024309.
[13] M. Tohyama, A.S. Umar, *Phys. Lett.* **B549** (2002) 72.
[14] P. Ring *et al.*, *Nucl. Phys.* **A722** (2003) 372c.
[15] O. Tarasov *et al.*, *Phys. Lett.* **B409** (1997) 64.
[16] Y. Utsuno, T. Otsuka, T. Mizusaki, M. Honma, *Phys. Rev.* **C60** (1999) 054315.
[17] T. Otsuka *et al.*, *Acta. Phys. Pol.* **B36** (2005) 1213.
[18] A.M. Bernstein et al., *Comments Nucl. Part. Phys.* **11** 203 (1983)
[19] J.K. Jewell et al., *Phys. Lett.* **B454** (1999) 181.
[20] G. Kraus *et al.*, *Phys. Rev. Lett* **73** (1994) 1773.
[21] S. Ottini-Hustache *et al.*, *Nucl. Instr. Meth. Phys. Res.* **A431** (1999) 476.
[22] L. Bianchi et al., Nucl. Inst. Meth. in Phys. Res. A276 (1989) 509.
[23] Y. Blumenfeld *et al.*, *Nucl. Instr. Meth. Phys. Res.* **A421** (1999) 471.
[24] A.J. Koning and J.P. Delaroche, *Nucl. Phys.* **A713** (2003) 231.
[25] F.D. Becchetti, G.W. Greenlees, *Phys. Rev.* **182** (1969) 1190.
[26] R.L. Varner et al., *Phys. Rep.* **201** (1991) 59.
[27] J. Raynal, *Phys. Rev.* **C23** (1981) 2571.
[28] P. Ring and P. Schuck, *The Nuclear Many-Body Problem* (Springer-Verlag, Berlin 1980).
[29] M. Grasso, N. Sandulescu, Nguyen Van Giai, R. J. Liotta, *Phys. Rev.* **C64** (2001) 064321.
[30] E. Chabanat, P. Bonche, P. Haensel, J. Meyer, R. Schaeffer, *Nucl. Phys.* **A635** (1998) 231.
[31] D.T. Khoa et al., *Nucl. Phys.* **A706** (2002) 61.
[32] J.P. Jeukenne, A. Lejeune and C. Mahaux, *Phys. Rev.* **C16** (1977) 80.
[33] T. Tamura W.R. Coker and F. Rybicki, *Comp. Phys. Comm.* **2** (1971) 94.
[34] R.S. Mackintosh, *Nucl. Phys.* **A209** (1973) 91.

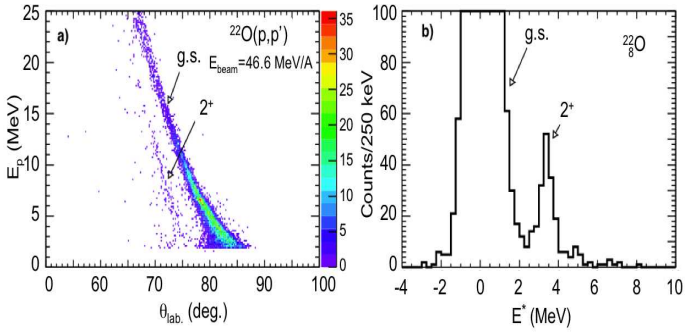

FIG. 1: a) : Scatterplot of recoiling proton energy versus scattering angle in the laboratory frame for the ^{22}O beam. b) : ^{22}O excitation energy spectrum deduced from the proton kinematics.

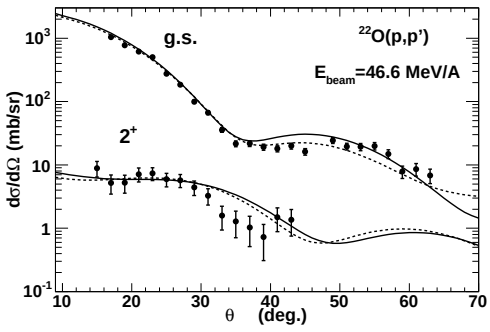

FIG. 2: Elastic and 2_1^+ inelastic angular distributions of ^{22}O at 46.6 A·MeV (dots). DWBA using the phenomenological KD global optical potential (solid lines), and folding model (dashed lines) calculations are shown (see text).